

\mathcal{PT} phase transition in multidimensional quantum systems

Carl M. Bender^{1*} and David J. Weir^{2†}

¹*Department of Physics, Kings College London, Strand, London WC2R 1LS, UK* [‡]

²*Blackett Laboratory, Imperial College, London SW7 2AZ, UK* [§]

Non-Hermitian \mathcal{PT} -symmetric quantum-mechanical Hamiltonians generally exhibit a phase transition that separates two parametric regions, (i) a region of unbroken \mathcal{PT} symmetry in which the eigenvalues are all real, and (ii) a region of broken \mathcal{PT} symmetry in which some of the eigenvalues are complex. This transition has recently been observed experimentally in a variety of physical systems. Until now, theoretical studies of the \mathcal{PT} phase transition have generally been limited to one-dimensional models. Here, four nontrivial coupled \mathcal{PT} -symmetric Hamiltonians, $H = \frac{1}{2}p^2 + \frac{1}{2}x^2 + \frac{1}{2}q^2 + \frac{1}{2}y^2 + igx^2y$, $H = \frac{1}{2}p^2 + \frac{1}{2}x^2 + \frac{1}{2}q^2 + y^2 + igx^2y$, $H = \frac{1}{2}p^2 + \frac{1}{2}x^2 + \frac{1}{2}q^2 + \frac{1}{2}y^2 + \frac{1}{2}r^2 + \frac{1}{2}z^2 + igxyz$, and $H = \frac{1}{2}p^2 + \frac{1}{2}x^2 + \frac{1}{2}q^2 + y^2 + \frac{1}{2}r^2 + \frac{3}{2}z^2 + igxyz$ are examined. Based on extensive numerical studies, this paper conjectures that all four models exhibit a phase transition. The transitions are found to occur at $g \approx 0.1$, $g \approx 0.04$, $g \approx 0.1$, and $g \approx 0.05$. These results suggest that the \mathcal{PT} phase transition is a robust phenomenon not limited to systems having one degree of freedom.

PACS numbers:

I. INTRODUCTION

We believe that in order to advance the theory of \mathcal{PT} quantum mechanics it is crucially important to answer the following natural question: Is there a \mathcal{PT} phase transition in higher-dimensional quantum systems, or is \mathcal{PT} quantum mechanics just limited to one-dimensional models?

Recently, there have been some modest attempts to study what happens when two \mathcal{PT} -symmetric systems are coupled and when a \mathcal{PT} -symmetric system is coupled to a conventionally Hermitian system (see, for example, Ref. [1]), but in these studies only trivial matrix and harmonic-oscillator models were considered. In early analytical approaches (see, for example, Refs. [2, 3]) some progress was made in calculating the \mathcal{C} operator for some complicated \mathcal{PT} -symmetric Hamiltonians; showing that the \mathcal{C} operator exists is equivalent to proving that the eigenvalues are real [4]. However, calculating the \mathcal{C} operator is difficult, and \mathcal{C} was only calculated to first order in perturbation theory in Refs. [2, 3].

In this paper we report a direct numerical attack on some nontrivial coupled Hamiltonians that were first considered in Ref. [3]. Specifically, we consider the four nontrivial

[‡] Permanent address: Department of Physics, Washington University, St. Louis, MO 63130, USA.

[§] Permanent address: Helsinki Institute of Physics, P.O. Box 64, University of Helsinki, 00014 Helsinki, Finland.

*Electronic address: cmb@wustl.edu

†Electronic address: david.weir03@imperial.ac.uk

Hamiltonians

$$H = \frac{1}{2}p^2 + \frac{1}{2}x^2 + \frac{1}{2}q^2 + \frac{1}{2}y^2 + igx^2y, \quad (1)$$

$$H = \frac{1}{2}p^2 + \frac{1}{2}x^2 + \frac{1}{2}q^2 + y^2 + igx^2y, \quad (2)$$

$$H = \frac{1}{2}p^2 + \frac{1}{2}x^2 + \frac{1}{2}q^2 + \frac{1}{2}y^2 + \frac{1}{2}r^2 + \frac{1}{2}z^2 + igxyz, \quad (3)$$

$$H = \frac{1}{2}p^2 + \frac{1}{2}x^2 + \frac{1}{2}q^2 + y^2 + \frac{1}{2}r^2 + \frac{3}{2}z^2 + igxyz, \quad (4)$$

where the coupling constants g are real parameters. For these Hamiltonians a convincing demonstration that there exists a range of g for which the eigenvalues are all real requires the accurate calculation of thousands of eigenvalues. Initial nondefinitive investigations using comparatively elementary numerical methods suggested that there might be complex eigenvalues for all nonzero values of g [5]. If this were true, then we would be forced to admit that \mathcal{PT} quantum mechanics is theoretically interesting but of limited scope.

This paper presents numerical evidence that for each of these complex Hamiltonians there are actually ranges of g for which the eigenvalues of these Hamiltonians are all real. Based on this numerical work, we conjecture that for H in (1) the critical value of g is about 0.1 and that when $|g| < 0.1$ the eigenvalues are *all* real. For the Hamiltonians in (2), (3), and (4) the critical values of g are about 0.04, 0.1, and 0.05, and when $|g|$ is less than these values, the eigenvalues are all real. To obtain these results we have used a powerful numerical scheme known as the *implicitly restarted Arnoldi method* [6]. We have calculated many thousands of eigenvalues accurate to about one part in 10^6 and have used about 20,000 hours of CPU time. Our results suggest that \mathcal{PT} quantum mechanics is general and robust, and that it extends to genuinely nontrivial higher-dimensional quantum-mechanical models. At present we can only draw conclusions based on detailed numerical studies, but the results in this paper suggest that \mathcal{PT} symmetry may even extend to infinite-dimensional quantum-field-theoretic models.

This paper is organized simply. In Sec. II we describe the \mathcal{PT} phase transition and in Sec. III we summarize our numerical approach and present our results in graphical form. Section IV contains brief concluding remarks.

II. \mathcal{PT} PHASE TRANSITION

A Hamiltonian is \mathcal{PT} symmetric if it is invariant under combined space reflection (parity) \mathcal{P} and time reversal \mathcal{T} . Such a Hamiltonian is said to have an *unbroken* \mathcal{PT} symmetry if its eigenfunctions are also eigenstates of the \mathcal{PT} operator. When the \mathcal{PT} symmetry of a Hamiltonian is unbroken, its eigenvalues are all real even though the Hamiltonian may not be Dirac Hermitian [7]. (We use the term *Dirac Hermitian* to describe a linear operator that remains invariant under the combined operations of matrix transposition and complex conjugation.) Such a \mathcal{PT} -symmetric Hamiltonian is physically relevant because it generates unitary time evolution [4].

\mathcal{PT} -symmetric Hamiltonians usually depend on one or more parameters. The Hamiltonians that have been studied so far typically possess an unbroken- \mathcal{PT} -symmetric phase (a parametric region of unbroken \mathcal{PT} symmetry in which all of the eigenvalues are real) and a broken- \mathcal{PT} -symmetric phase (a parametric region of broken \mathcal{PT} symmetry in which some of the eigenvalues are complex). The boundary between these two regions is the \mathcal{PT} phase transition and this transition occurs at a critical value of a parameter.

A simple example of a \mathcal{PT} -symmetric Hamiltonian that has a \mathcal{PT} phase transition is the 2×2 matrix Hamiltonian [8]

$$H = \begin{pmatrix} re^{i\theta} & s \\ s & re^{-i\theta} \end{pmatrix}, \quad (5)$$

where the three parameters r , s , and θ are real. This Hamiltonian is not Dirac Hermitian but it is \mathcal{PT} invariant, where the parity operator \mathcal{P} is

$$\mathcal{P} = \begin{pmatrix} 0 & 1 \\ 1 & 0 \end{pmatrix} \quad (6)$$

and the time-reversal operator \mathcal{T} is complex conjugation. The region of unbroken \mathcal{PT} symmetry is $s^2 \geq r^2 \sin^2 \theta$.

Almost all studies of non-Hermitian \mathcal{PT} -symmetric quantum-mechanical Hamiltonians have focused on finite-dimensional matrix Hamiltonians like that in (5) or on one-degree-of-freedom Hamiltonians of the type $H = p^2 + V(x)$, for which the condition of \mathcal{PT} symmetry is $V^*(x) = V(-x)$. The Schrödinger eigenvalue problem $H\psi = E\psi$ for such Hamiltonians takes the form of the ordinary differential equation $-\psi''(x) + V(x)\psi(x) = E\psi(x)$.

The first \mathcal{PT} -symmetric Hamiltonian that was studied in detail has the form

$$H = p^2 + x^2(ix)^\varepsilon, \quad (7)$$

where ε is a real parameter [9, 10]. Dorey, Dunning, and Tateo proved that the eigenvalues of the corresponding Schrödinger eigenvalue equation

$$-\psi''(x) + x^2(ix)^\varepsilon\psi(x) = E\psi(x) \quad (8)$$

are all real when $\varepsilon \geq 0$ [11, 12]. These eigenvalues are plotted as functions of ε in Fig. 1. The critical value of ε is 0, and the region of broken \mathcal{PT} symmetry is $\varepsilon < 0$. As ε approaches 0 through negative values, complex-conjugate pairs of eigenvalues become degenerate as they emerge from the complex plane and then split into real pairs of eigenvalues. The values of ε at which the eigenvalues become degenerate are sometimes called *exceptional points* [13]. Observe from Fig. 1 that $\varepsilon = 0$ is the *limit point* of a sequence of exceptional points. For this model the decomplexification process is a high-energy phenomenon; that is, as ε approaches 0 from below, sequentially higher eigenvalues (rather than lower eigenvalues) become degenerate. This is because ε is a *singular* perturbation parameter [14]. (The same kind of limiting process was discovered many years ago for the case of the anharmonic oscillator $H = p^2 + x^2 + gx^4$, except that for the anharmonic oscillator the exceptional points lie in the complex- g plane rather than on the real- g axis [14, 15].)

Many other \mathcal{PT} -symmetric Hamiltonians that exhibit \mathcal{PT} phase transitions have been studied. For example, the Hamiltonian

$$H = p^2 + x^4 + iAx, \quad (9)$$

where A is a real parameter, exhibits a \mathcal{PT} phase transition at $A = \pm 3.169$ [16]. In contrast to the Hamiltonian (7), as A approaches the phase transition through the region $|A| > 3.169$ of broken \mathcal{PT} symmetry, the eigenvalues emerge from the complex domain starting with the highest-lying eigenvalues and ending with the lowest-lying eigenvalues. The exceptional points remain well separated and do not converge to a limit point because A is a *regular* perturbation parameter [14].

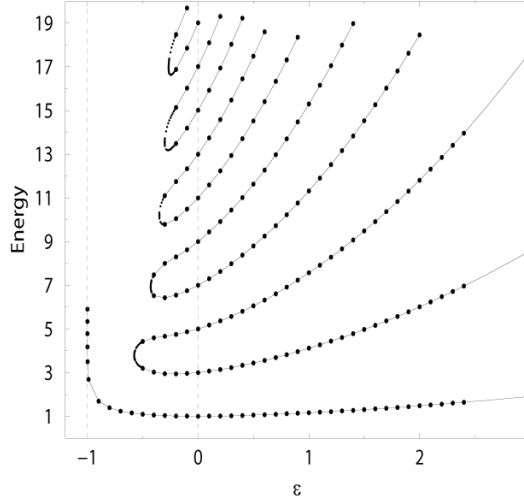


FIG. 1: Real eigenvalues of the \mathcal{PT} -symmetric Hamiltonian (7) plotted as functions of ε . The region of unbroken \mathcal{PT} symmetry is $\varepsilon \geq 0$. In the region $\varepsilon < 0$ of broken \mathcal{PT} symmetry, the eigenvalues emerge from the complex plane at exceptional points as degenerate pairs; these pairs then split into real eigenvalues. As ε approaches the critical point at 0 from below, this decomplexification process begins with the low-lying eigenvalues and terminates at $\varepsilon = 0$ at the highest-lying eigenvalues.

Another example of a \mathcal{PT} -symmetric Hamiltonian having a \mathcal{PT} phase transition is

$$H = -\frac{d^2}{d\theta^2} + ig \cos \theta, \quad (10)$$

where g is a real parameter [17]. Here, the Schrödinger eigenvalue problem is posed on a finite rather than on an infinite domain. If the eigenfunctions are required to be 2π periodic and odd in θ , the region of unbroken \mathcal{PT} symmetry is $|g| < 3.4645$ [17].

A physically motivated example of a \mathcal{PT} -symmetric Hamiltonian that exhibits a \mathcal{PT} phase transition was discussed by Rubinstein, Sternberg, and Ma [18]. Their Hamiltonian arises in the context of superconducting wires. Again, the Schrödinger eigenvalue problem

$$-\psi''(x) - igx\psi(x) = E\psi(x) \quad (11)$$

is posed on the finite domain $|x| \leq 1$ and the boundary conditions are $\psi(\pm 1) = 0$. The region of unbroken \mathcal{PT} symmetry is $g < 12.31$, and the behavior of the eigenvalues is qualitatively similar to that of H in (10). (Compare Fig. 1 of Ref. [17] with Fig. 1 of Ref. [18].)

The \mathcal{PT} phase transition has been seen repeatedly in laboratory experiments. It was first observed in optical wave guides [19–23], but it has also been observed in atomic diffusion [24], lasers [25, 26], superconducting wires [18], nuclear magnetic resonance [27], and most recently in microwave cavities [28] and in electronic circuits [29]. The \mathcal{PT} phase transition is a clear and prominent effect and not a subtle phenomenon; laboratory measurements and theoretical predictions have agreed with virtually no error.

Theoretical studies of eigenvalues (as in Fig. 1) and experimental observations suggest that the \mathcal{PT} phase transition is quite generic, but almost all of the theoretical and experimental work that has been done so far has concerned systems that have just one degree of freedom. Indeed, the proof of the reality of the eigenvalues in Refs. [11, 12] relies on

establishing a correspondence, known as the *ODE/IM correspondence*, between ordinary differential equations and integrable models. We emphasize that this correspondence involves *ordinary* and not *partial* differential equations. Thus, we are motivated to study in Sec. III the eigenvalues of the four multidimensional Hamiltonians in (1) - (4).

III. NUMERICAL CALCULATION OF EIGENVALUES

To find the eigenvalues of the Hamiltonians in (1) - (4), we follow a calculational approach that was used in Ref. [10]. We express the Hamiltonian in harmonic-oscillator-basis states [see Eq. (3.2) in Ref. [10]], truncate the Hamiltonian matrix to an $N \times N$ numerical array, and then calculate the eigenvalues. In this paper the eigenvalues are calculated using the implicitly restarted Arnoldi method as implemented by ARPACK [30]. This numerical technique works particularly well because the array is *sparse*; that is, only a small percentage of the matrix elements are nonzero. Furthermore, the matrix becomes increasingly sparse with increasing dimension.

As is shown in Fig. 12 of Ref. [10], the convergence of the eigenvalues as N increases is noisy at first, but starting with the lowest energies, the eigenvalues settle down one-by-one to their correct limiting values. In Ref. [10] the eigenvalues of the Hamiltonian $H = p^2 + ix^3$ are calculated as the dimension of the matrix ranges up to $N = 15$. Here, to illustrate the convergence of the eigenvalues, we plot in Fig. 2 the eigenvalues of

$$H = p^2 + x^2 + ix^3 \quad (12)$$

for N ranging from 2 to 100. Note that the eigenvalues are converging to the values shown in Fig. 1 for $\varepsilon = 1$.

A. Calculation of the Eigenvalues of the Hamiltonian (1)

If we use the same approach for H in (1), the numerical convergence is *faster* than that for H in (12) because the matrix is more sparse; only about 5% of the matrix elements are nonzero. Using $100^2 \times 100^2$ matrices (10^8 matrix elements), we calculate the eigenvalues for g ranging from 0 to 0.4 in steps of 0.0005. There are 10^4 eigenvalues, but we limit our attention to those eigenvalues that have settled down and are changing by less than one part in 10^6 as we increase the size of the matrix from $80^2 \times 80^2$ to $90^2 \times 90^2$ to $100^2 \times 100^2$. In Figs. 3 and 4 we plot the real and imaginary parts of those eigenvalues whose real parts range from 0 to 16. A key result is given in Fig. 4; it appears that for g greater than about 0.1 there are many complex eigenvalues, but that there are no complex eigenvalues when $g < 0.1$. This suggests that there is a critical value of g near 0.1.

From the eigenvalues in Fig. 4 we then select out just the eigenvalues that have nonzero imaginary parts. The real parts of these eigenvalues are shown in Fig. 5. Note that the real parts of these eigenvalues increase rapidly as g decreases. Thus, if there is a nonzero critical value of g at which a \mathcal{PT} phase transition occurs, this transition is a high-energy phenomenon, as opposed to the \mathcal{PT} phase transition of H in (7) (see Fig. 1).

If we trace a curve through the left-most points in Fig. 5, we can see that this curve rises steeply as g decreases, and we believe that this curve becomes infinite at approximately $g \approx 0.1$. Unfortunately, it is not easy to fit a curve numerically through these points because they are not very regular. However, when we repeat these numerical calculations

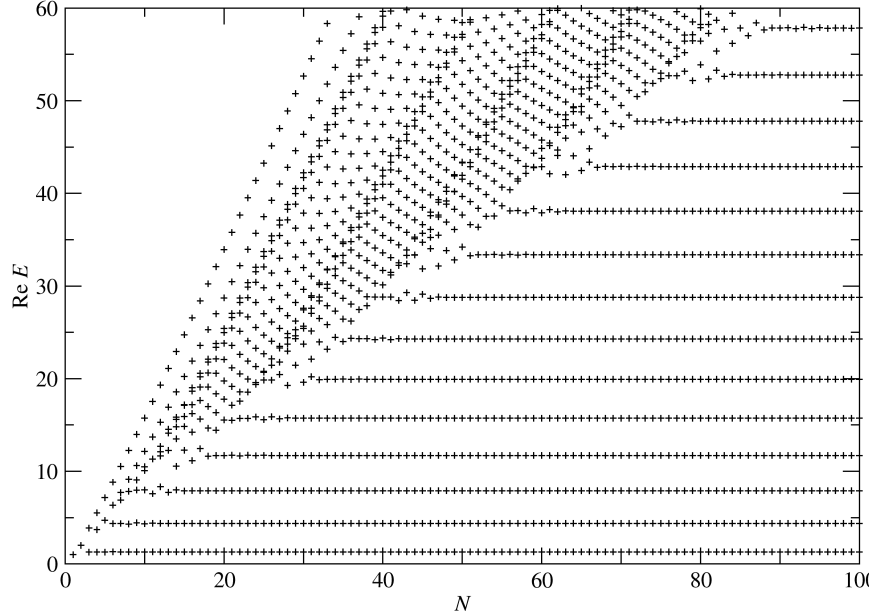


FIG. 2: Numerical convergence of the first seven eigenvalues of the Hamiltonian in (12) using the implicitly restarted Arnoldi method. At first, the eigenvalues vary chaotically as the dimension N of the matrix increases, but eventually, starting with the lowest energies, they settle down to their correct numerical values as shown in Fig. 1 at $\varepsilon = 1$.

for the Hamiltonian (2), we find that the corresponding points are more regular, and it is indeed possible to fit such a curve.

B. Calculation of the Eigenvalues of the Hamiltonian (2)

For the Hamiltonian (2), we construct Figs. 6 and 7, which are the analogs of Figs. 3 and 4. Note that the eigenvalues no longer show a breaking of degeneracy as g increases from 0. In Fig. 7 we plot the imaginary parts of those eigenvalues. Note that there are no complex eigenvalues when g is below about 0.08.

From the eigenvalues in Fig. 6 we select out just the eigenvalues that have nonzero imaginary parts. The real parts of these eigenvalues are shown in Fig. 8. As in the case of Fig. 5, these real parts increase rapidly as g decreases.

Because the left-most points in Fig. 8 are quite regular, we can numerically fit a curve that passes approximately through these points. If we seek a curve of the form

$$f(g) = a(g - b)^c, \quad (13)$$

we find that

$$a = 2.32 \pm 0.18, \quad b = 0.046 \pm 0.002, \quad c = -0.615 \pm 0.033. \quad (14)$$

If we then try a more elaborate curve of the form

$$f(g) = a(g - b)^c [-\log(g - b)]^d,$$

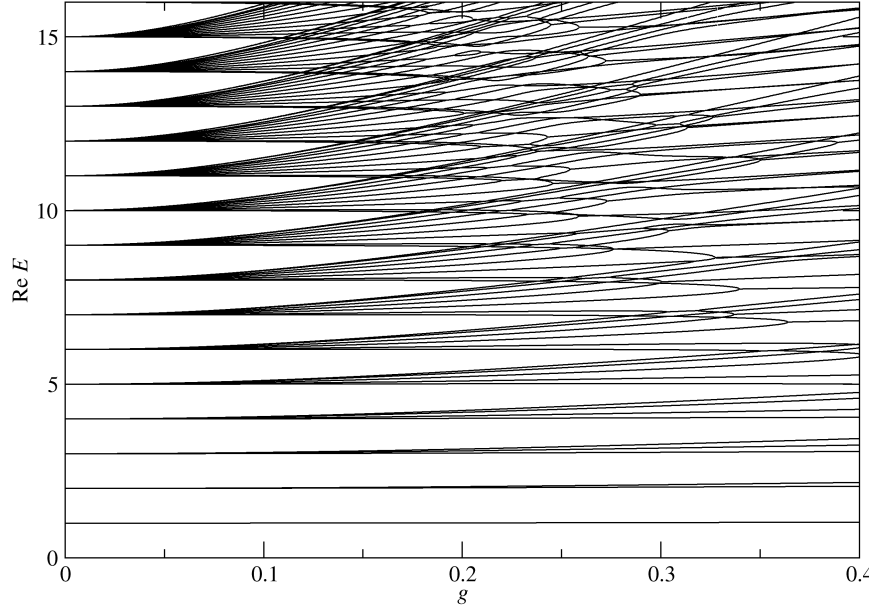


FIG. 3: Real parts of the eigenvalues of H in (1) that have converged for a $100^2 \times 100^2$ matrix plotted versus g . The coupling constant g ranges from 0 to 0.4 in steps of 0.0005, and the eigenvalues shown have real parts less than 16. The plot is complicated because when $g = 0$ the eigenvalues become increasingly degenerate with increasing energy; there is one eigenvalue of energy 1, two eigenvalues of energy 2, three eigenvalues of energy 3, and so on. As g increases, the degeneracy is broken. Eventually, one can see energy levels crossing, but most crossings only represent accidental degeneracies. One must look carefully to see the exceptional points, which are not so easy to see as those in Fig. 1. In the range of g shown, the lowest-energy exceptional point occurs at about $g = 0.364$, where one of the sixth and one of the seventh eigenvalues become degenerate and form a complex-conjugate pair.

we find that the value of c is consistent with 0, which suggests an improved fitting curve of the form

$$f(g) = a[-\log(g - b)]^d. \quad (15)$$

The numerical fit then gives

$$a = 2.17 \pm 0.11, \quad b = 0.054 \pm 0.001, \quad d = 1.67 \pm 0.5. \quad (16)$$

Thus, based on these extrapolations, we are moderately confident that there is a critical value of g near 0.05, which is somewhat smaller than the rough estimate of g_{crit} obtained by inspection of Fig. 7.

C. Calculation of the Eigenvalues of the Hamiltonian (3)

Next we consider the Hamiltonian H in (3). We diagonalize a $30^3 \times 30^3$ matrix representation of H and plot the results in Figs. 9 and 10. Figure 10 suggests that there is a \mathcal{PT} phase transition near $g \approx 0.25$. These eigenvalues have stopped changing as the size of the

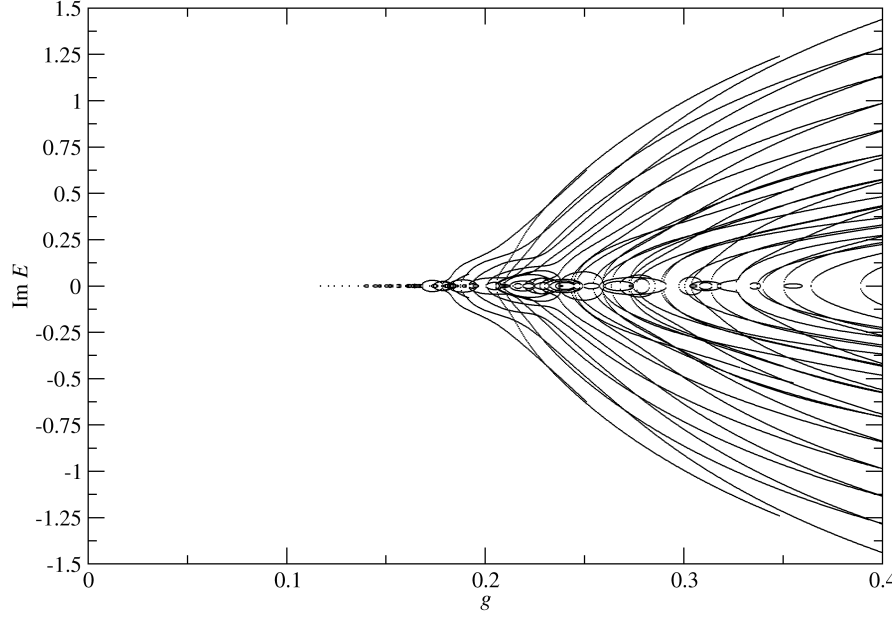


FIG. 4: Imaginary parts of the eigenvalues whose real parts are shown in Fig. 3. Note that the imaginary parts of the eigenvalues are much smaller than the real parts by roughly a factor of 10. For the size of the matrix studied, it appears that the critical point is at $g \approx 0.1$. Below this point there are no complex eigenvalues whose real parts are less than 16.

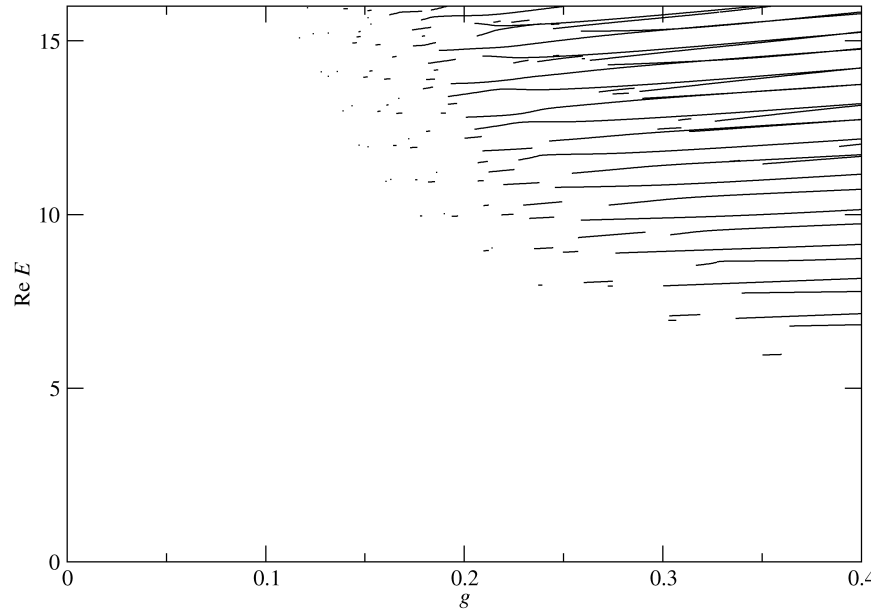


FIG. 5: Real parts of the eigenvalues in Fig. 4 whose imaginary parts are nonzero. Note that the real parts of these eigenvalues grow with decreasing g . We can obtain a more accurate estimate of the critical value of g by tracing a curve through the left-most points on the graph.

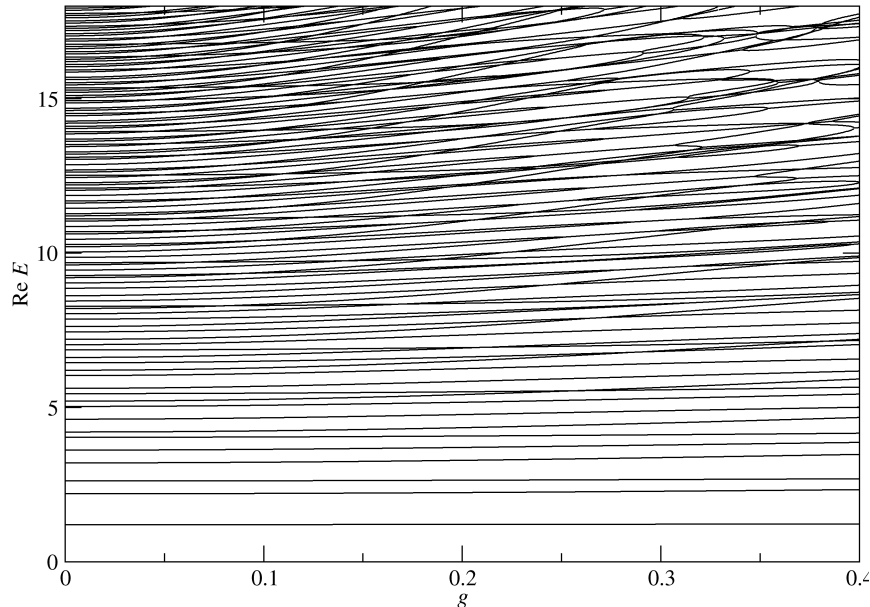


FIG. 6: Real parts of the eigenvalues of the \mathcal{PT} -symmetric Hamiltonian (2) plotted as functions of g for $0 \leq g \leq 0.4$ in steps of 0.0005. All eigenvalues (both real and complex) whose real parts are less than 18 are shown. This graph is the analog of Fig. 3.

matrix size increases from $20^3 \times 20^3$ to $25^3 \times 25^3$ to $30^3 \times 30^3$. Then, in Fig. 11 we isolate just those eigenvalues whose nonzero imaginary parts are shown in Fig. 10.

D. Calculation of the Eigenvalues of the Hamiltonian (4)

The analogs of Figs. 9 and 10 for the Hamiltonian (4) are Figs. 12 and 13. However, because the eigenvalue degeneracies have been lifted, the left-most points in Fig. 14 are regular enough to perform fits of the form in (13) and (15). The first fit gives the value 0.049 ± 0.001 for the critical point and the second fit gives a value of 0.064 ± 0.001 for the critical point. Thus, we may estimate that there is a critical value of g near 0.057, which is somewhat smaller than what one would guess from Fig. 13.

IV. SUMMARY

We have presented extensive numerical evidence in this paper that suggests that the eigenvalues of the multidimensional trilinear Hamiltonians (1–4) are entirely real when the coupling constant g is less than a critical value. If this numerical evidence stands up to further study, then we can conclude that these quantum theories possess an unbroken \mathcal{PT} -symmetric phase for sufficiently small g and display a transition to a broken phase as g increases. This would suggest that multidimensional \mathcal{PT} -symmetric quantum systems can exhibit the same kind of phase transition that one-dimensional quantum systems are known to exhibit. On the basis of this work we are tempted to conjecture that even \mathcal{PT} -symmetric quantum field theories such as an $ig\phi^3$ theory might exhibit a \mathcal{PT} phase transition as the

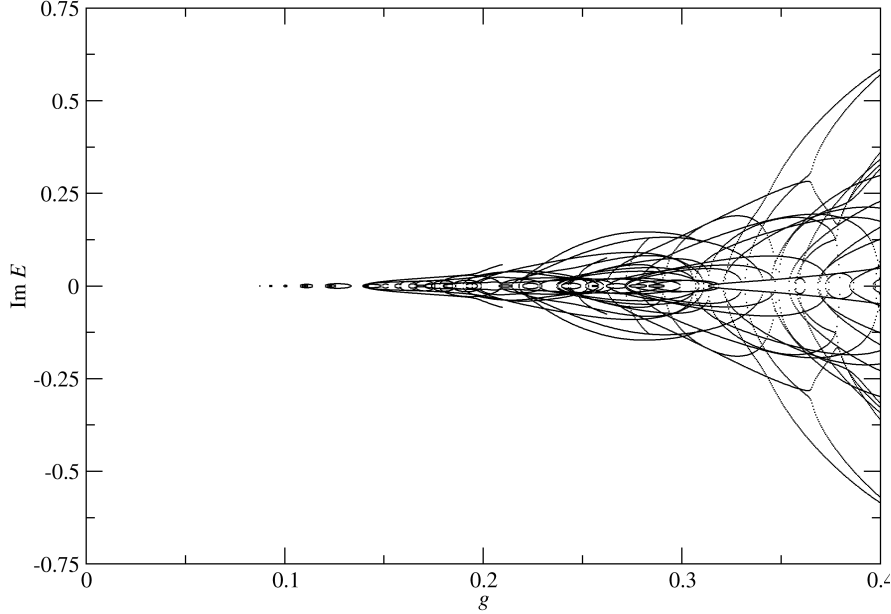


FIG. 7: Imaginary parts of the eigenvalues whose real parts are shown in Fig. 6. Note that the imaginary parts of the eigenvalues are smaller than the real parts by a factor of roughly 10. For the size of the matrix studied, it appears that the critical point is near $g \approx 0.08$. Below this point we see no complex eigenvalues whose real parts are less than 18. Further analysis (see Fig. 8) suggests that the critical point is near 0.05.

coupling constant g increases from 0.

In this paper we have only considered cubic and trilinear interactions because the harmonic-oscillator-basis functions that we have used to construct the large numerical matrices whose eigenvalues we have obtained numerically have exponentially vanishing asymptotic behaviors on the real axis. It would be interesting to study quartic Hamiltonians using similar techniques, but we anticipate that the numerical analysis would be much more difficult because the harmonic-oscillator-basis functions and the exact eigenfunctions have very different asymptotic behaviors on the real axis.

Finally, we mention again that if there really is a \mathcal{PT} -symmetric phase transition for the models that we have studied, this transition is generically a high-energy phenomenon. Unfortunately, this presents a severe problem for the numerical techniques used in this paper because the Arnoldi method can only give detailed information about converged eigenvalues for low energies as the size of the matrix is increased. Thus, the principal finding in this paper, namely, that the models we have studied exhibit a \mathcal{PT} phase transition, can only be conjectural in nature.

Acknowledgments

CMB is supported by the U.K. Leverhulme Foundation and by the U.S. Department of Energy. DJW thanks the Imperial College High Performance Computing Service for the use

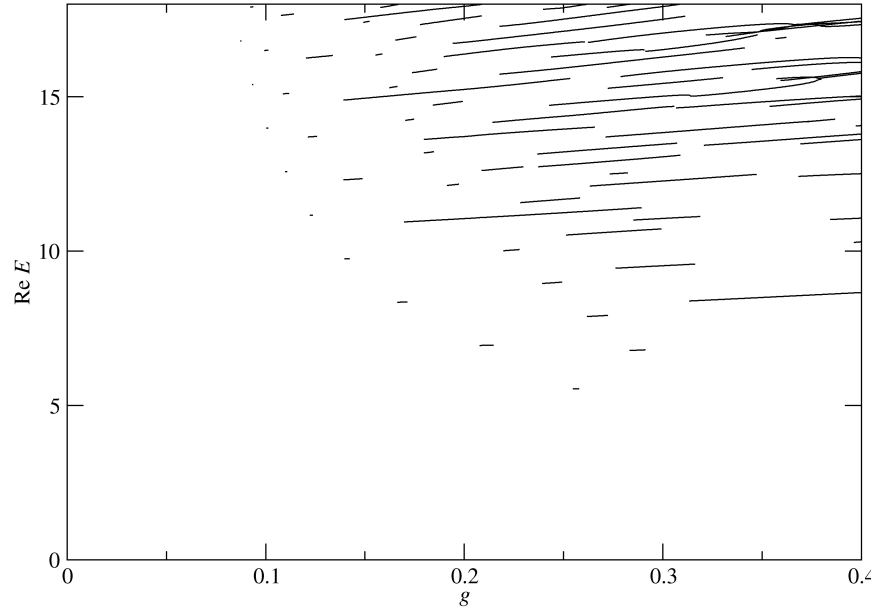


FIG. 8: Real parts of the eigenvalues in Fig. 6 whose imaginary parts are nonzero; the real parts of these eigenvalues grow with decreasing g . We can obtain a more accurate determination of the critical value of g by fitting a curve through the left-most points on the graph, which are much more regular than the left-most points in the analogous Fig. 5.

of its resources.

-
- [1] C. M. Bender and H. F. Jones, J. Phys. A: Math. Theor. **41**, 244006 (2008).
 - [2] C. M. Bender, D. C. Brody, and H. F. Jones, Phys. Rev. Lett. **93**, 251601 (2004); C. M. Bender, I. Cavero-Pelaez, K. A. Milton, and K. V. Shajesh, Phys. Lett. B **613**, 97 (2005).
 - [3] C. M. Bender, J. Brod, A. Refig, and M. E. Reuter, J. Phys. A: Math. Gen. **37**, 10139-10165 (2004).
 - [4] C. M. Bender, D. C. Brody, and H. F. Jones, Phys. Rev. Lett. **89**, 270401 (2002).
 - [5] We thank Q. Wang for a discussion of this point.
 - [6] R. B. Lehoucq and D. C. Sorensen, SIAM J. Matrix Anal. & Appl. **17**, 789 (1996).
 - [7] C. M. Bender, Contemp. Phys. **46**, 277 (2005) and Repts. Prog. Phys. **70**, 947 (2007).
 - [8] C. M. Bender, D. C. Brody, and H. F. Jones, Am. J. Phys. **71**, 1095-1102 (2003).
 - [9] C. M. Bender and S. Boettcher, Phys. Rev. Lett. **80**, 5243 (1998).
 - [10] C. M. Bender, S. Boettcher, and P. N. Meisinger, J. Math. Phys. **40**, 2201 (1999).
 - [11] P. Dorey, C. Dunning, and R. Tateo, J. Phys. A: Math. Gen. **34**, L391 (2001) and **34**, 5679 (2001).
 - [12] P. Dorey, C. Dunning, and R. Tateo, J. Phys. A: Math. Gen. **40**, R205 (2007).
 - [13] An early use of WKB to locate critical (exceptional) points may be found in C. M. Bender and T. T. Wu, Phys. Rev. Lett. **21**, 406 (1968) and Phys. Rev. **184**, 1231 (1969). For more recent theoretical and experimental studies of exceptional points see W. D. Heiss, Czech. J. Phys. **54**,

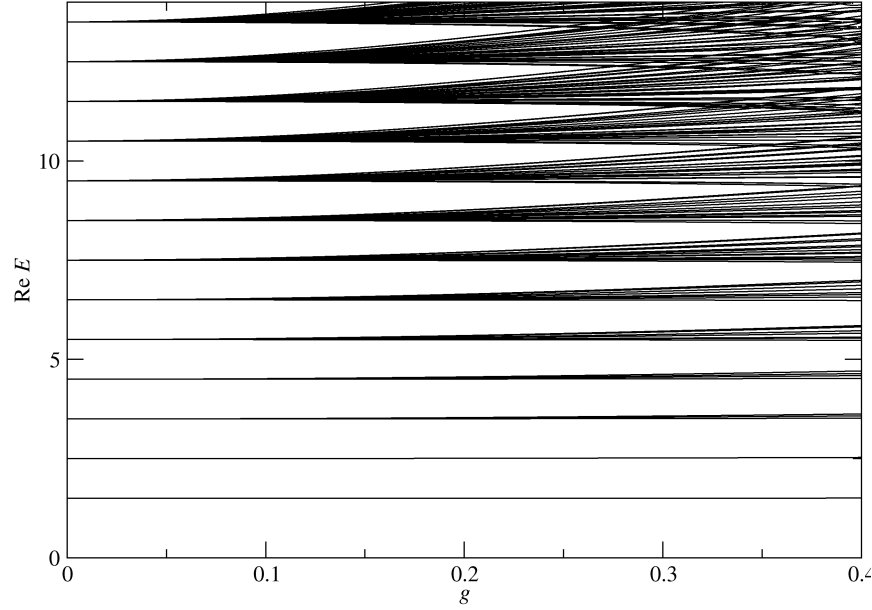


FIG. 9: Real parts of the eigenvalues of H in (3) that have converged for a $30^3 \times 30^3$ matrix plotted versus g . The coupling constant g ranges from 0 to 0.4 in steps of 0.0005, and the eigenvalues shown have real parts less than 14. The plot is complicated because when $g = 0$ the eigenvalues become increasingly degenerate with increasing energy. There is one eigenvalue of energy 1.5, three of energy 2.5, six of energy 3.5, ten of energy 4.5, and so on. As g increases, the degeneracy is broken. Eventually, one can see energy levels crossing, but as in Fig. 3, most crossings only represent accidental degeneracies. It is very difficult to find the exceptional points.

- 1091 (2004); B. Dietz, H. L. Harney, O. N. Kirillov, M. Miski-Oglu, A. Richter, and F. Schäfer, Phys. Rev. Lett. **106**, 150403 (2011); A. Andrianov and A. V. Sokolov, SIGMA **7**, 111 (2011), and references therein; M. Fagotti, C. Bonatti, D. Logoteta, P. Marconcini, and M. Macucci, Phys. Rev. B **83**, 241406 (R) (2011).
- [14] C. M. Bender and S. A. Orszag, *Advanced Mathematical Methods for Scientists and Engineers* (McGraw Hill, New York, 1978), Chap. 7.
- [15] C. M. Bender and T. T. Wu, Phys. Rev. Lett. **21**, 406 (1968) “Analytic Structure of Energy Levels in a Field-Theory Model” and Phys. Rev. **184**, 1231 (1969).
- [16] C. M. Bender, M. Berry, P. N. Meisinger, V. M. Savage, and M. Şimşek, J. Phys. A: Math. Gen. **34**, L31-L36 (2001).
- [17] C. M. Bender and R. J. Kalveks, Int. J. Theor. Phys. **50**, 955 (2011).
- [18] J. Rubinstein, P. Sternberg, and Q. Ma, Phys. Rev. Lett. **99**, 167003 (2007).
- [19] Z. Musslimani, K. Makris, R. El-Ganainy, and D. Christodoulides, Phys. Rev. Lett. **100**, 030402 (2008).
- [20] K. Makris, R. El-Ganainy, D. Christodoulides, and Z. Musslimani, Phys. Rev. Lett. **100**, 103904 (2008).
- [21] A. Guo, G. J. Salamo, D. Duchesne, R. Morandotti, M. Volatier-Ravat, V. Aimez, G. A. Siviloglou, and D. N. Christodoulides, Phys. Rev. Lett. **103**, 093902 (2009).
- [22] C. E. Rüter, K. G. Makris, R. El-Ganainy, D. N. Christodoulides, M. Segev, and D. Kip,

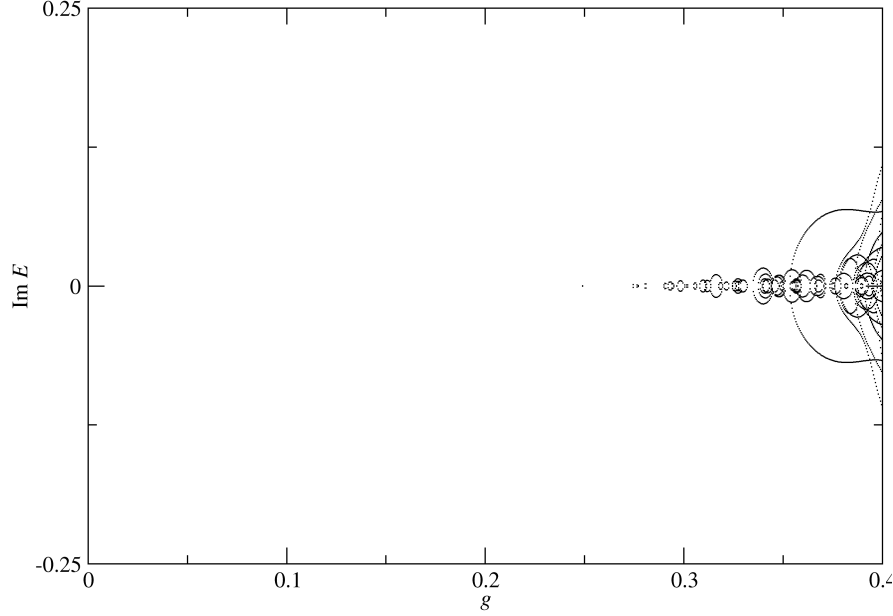


FIG. 10: Imaginary parts of the eigenvalues whose real parts are shown in Fig. 9. There appears to be a critical point at $g \approx 0.25$. Below this point there are no complex eigenvalues at all. The eigenvalue behavior shown in this figure is similar to that shown in Figs. 4 and 7 for the Hamiltonians in (1) and (2).

Nat. Phys. **6**, 192-195 (2010).

- [23] L. Feng, M. Ayace, J. Huang, Y.-L. Xu, Y.-F. Chen, Y. Fainman, and A. Scherer, Science **333**, 729 (2011).
- [24] K. F. Zhao, M. Schaden, and Z. Wu, Phys. Rev. A **81**, 042903 (2010).
- [25] Y. D. Chong, L. Ge, and A. D. Stone, Phys. Rev. Lett. **106**, 093902 (2011).
- [26] Z. Lin, H. Ramezani, T. Eichelkraut, T. Kottos, H. Cao, and D. N. Christodoulides, Phys. Rev. Lett. **106**, 213901 (2011).
- [27] C. Zheng, L. Hao, and G. L. Long, arXiv:1105.6157 [quant-ph].
- [28] S. Bittner, B. Dietz, U. Guenther, H. L. Harney, M. Miski-Oglu, A. Richter, and F. Schaefer, Phys. Rev. Lett. **108**, 024101 (2012).
- [29] J. Schindler, A. Li, M. C. Zheng, F. M. Ellis, T. Kottos, Phys. Rev. A **84**, 040101 (2011).
- [30] R. B. Lehoucq, D. C. Sorensen, and C. Yang, *ARPACK Users' Guide* (SIAM, New York, 1998).

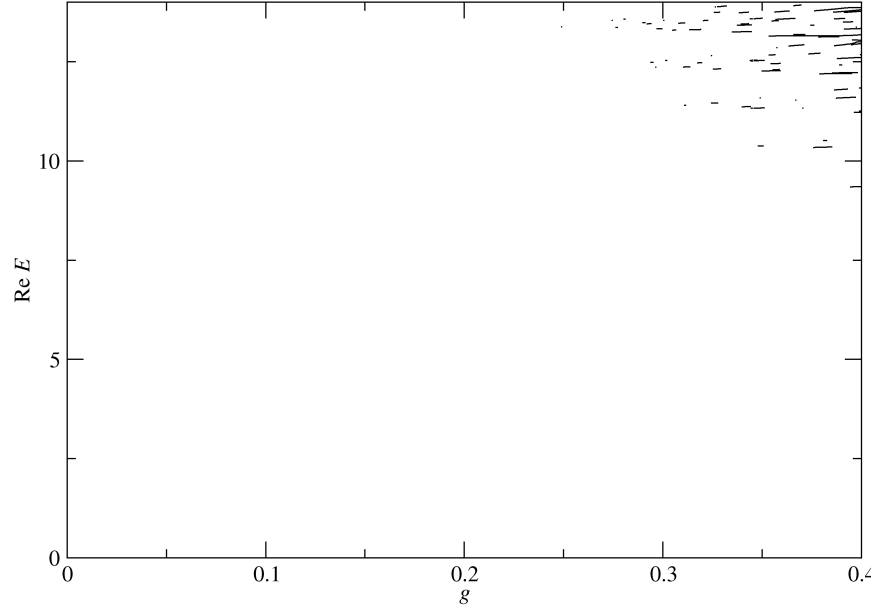


FIG. 11: Real parts of the eigenvalues in Fig. 9 whose imaginary parts are nonzero. Note that the real parts of these eigenvalues grow with decreasing g . We can try to obtain a more accurate determination of the critical value of g by tracing a curve through the left-most points on the graph and estimating that this curve blows up near $g \approx 0.2$. Unfortunately these points are not regular enough to do a numerical fit to such a curve.

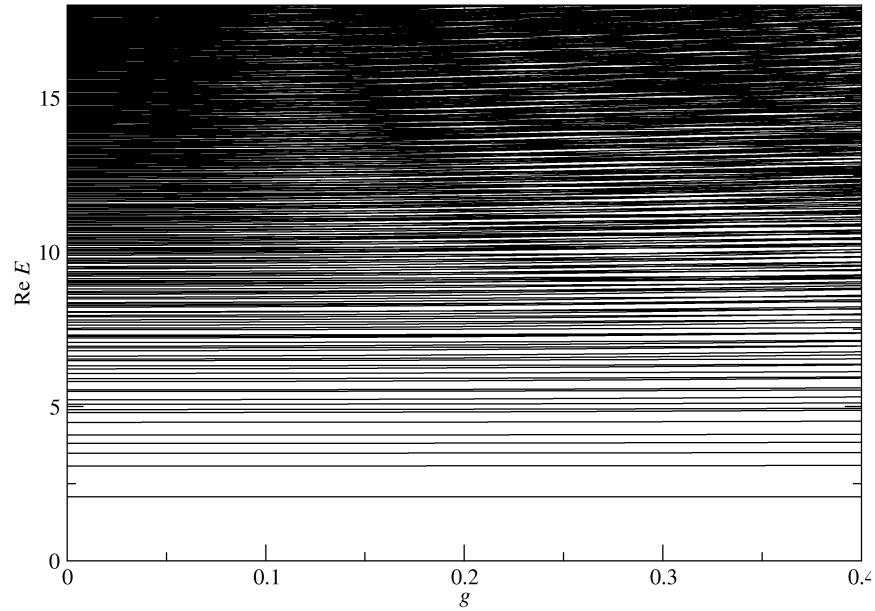


FIG. 12: Real parts of the eigenvalues of the \mathcal{PT} -symmetric Hamiltonian (4) plotted as functions of g for g ranging from 0 to 0.4 in steps of 0.0005. All eigenvalues (both real and complex) whose real parts are less than 18 are shown.

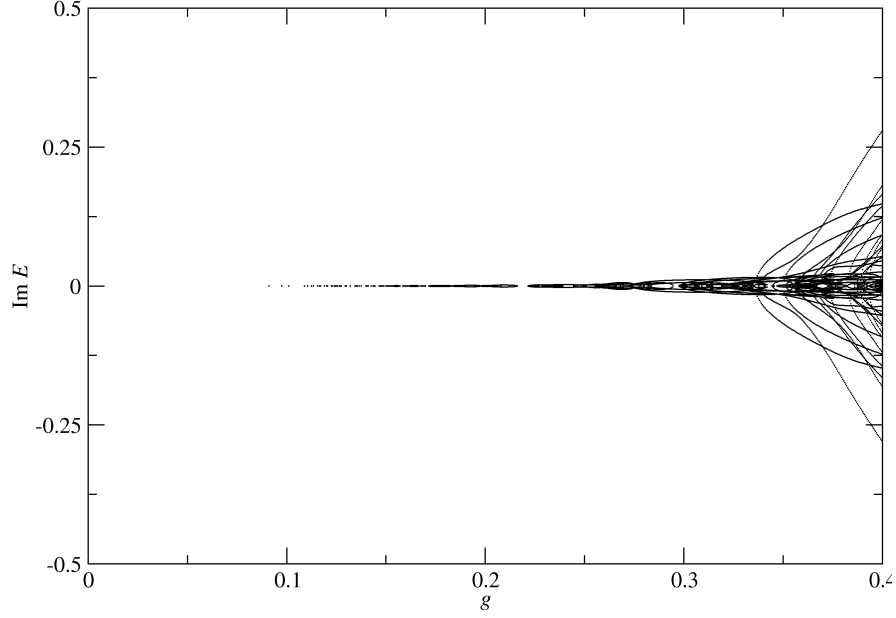


FIG. 13: Imaginary parts of the eigenvalues whose real parts are shown in Fig. 12. There appears to be a critical point near $g \approx 0.09$. Below this point there are no complex eigenvalues in the range studied. Further analysis (see Fig. 14) suggests that the critical value of g is near 0.057. The eigenvalue behavior shown in this figure is similar to that shown in Figs. 4, 7, and 10 for the Hamiltonians in (1–3).

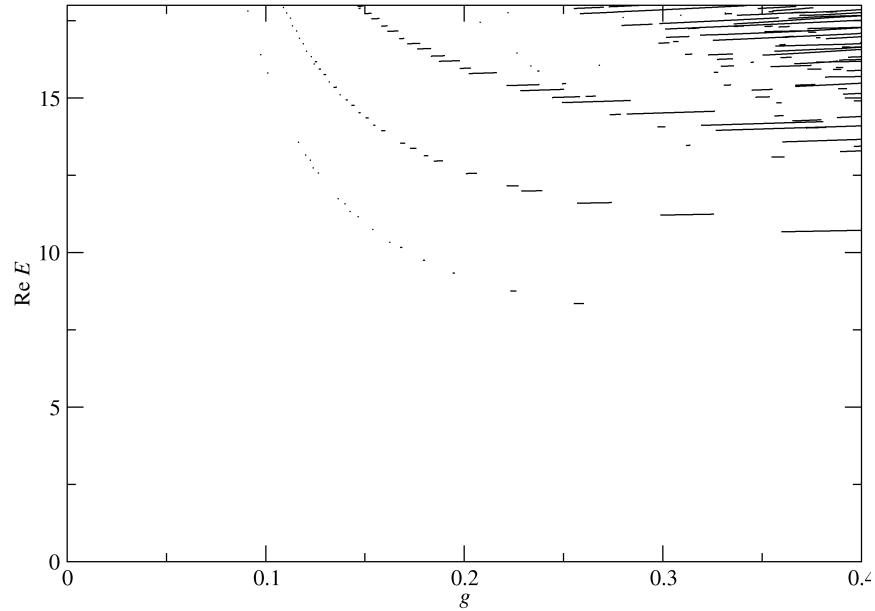


FIG. 14: Real parts of the eigenvalues in Fig. 12 whose imaginary parts are nonzero. These eigenvalues grow with decreasing g . A numerical fit to the left-most points on the graph predicts that the critical value of g is about 0.05.